Hydro-mechanical Energy Storage System for Hydrostatic Transmissions in Mobile Machinery

Dipl.-Ing. Felix Straßburger

Institute for Machine Elements and Machine Design (IME), RWTH Aachen University, Schinkelstr. 10, 52056 Aachen, Germany. E-mail: strassburger@ime.rwth-aachen.de

Univ.-Prof. Dr.-Ing. Georg Jacobs

Institute for Machine Elements and Machine Design (IME), RWTH Aachen University, Schinkelstr. 10, 52056 Aachen, Germany. E-mail: jacobs@ime.rwth-aachen.de

Abstract

Due to their frequent acceleration and deceleration cycles, industrial trucks and mobile machines offer strong potential for reduction of both fuel consumption and emissions through energy recuperation mechanisms. Simulation results show that fuel savings of up to 14% can be expected as a result of using brake energy recuperation in the field of hydrostatically driven industrial trucks. A hybrid system for hydrostatic drives is currently being developed, constructed and tested at the Institute for Machine Elements and Machine Design (IME). The hybrid system is constructed in the form of a hydro-mechanical storage system consisting of an adjustable axial piston unit providing input and output and a flywheel for energy storage. This provides an effective recuperation mechanism for hydrostatic drive systems, combining the benefits of high power and high energy density.

KEYWORDS: hydrostatic drive, hybrid, industrial truck, fuel consumption reduction, flywheel storage

1 Introduction

Recuperation of the kinetic energy that is stored in a moving vehicle offers an effective approach to obtain significant reductions in the emissions from industrial trucks and mobile machinery. In conventional powertrains, the kinetic energy stored in the vehicle is converted into heat during braking. Due to the need for many types of mobile machines and industrial vehicles to be frequently operated in reverse, the savings available from recovery of kinetic energy are more pronounced than in passenger cars. For example, when the braking and acceleration patterns in the NEDC cycle used in the passenger car sector are compared with the VDI cycle specified by VDI Guideline

2198 for industrial trucks, the recuperation system is used six times as often every hour.

A conventional forklift with a maximum lifting capacity of 2 tonnes will be converted into a hybrid truck as part of a research project at the IME. The forklift is fitted with a hydrostatic transmission as standard. In a conventional hydrostatic drive, the deceleration of the vehicle is either effected by friction brakes or by the drag torque of the combustion engine. In addition, a load torque can be applied to the crankshaft, for example, by means of a throttle valve integrated into the power hydraulics. There is no additional friction brake integrated in the vehicle considered, meaning that all braking is purely hydraulic.

2 Vehicle modelling

The IME has developed a vehicle model comprising multiple model stages using the software AMESim. The first stage of the vehicle model includes the hydrostatic drive and the running resistances encountered during operation. In the second stage, the vehicle's internal combustion engine is also modelled in the simulation. In the third stage, the additional hybrid system is integrated into the drive train. The vehicle model is used for system design and analysis of power flows and losses. The later stages of the project make use of the vehicle model in conjunction with MATLAB/Simulink to develop the operating strategy. The plausibility of the simulation results from the first and second model layers were validated using measured data. **Figure 1** shows a comparison between the measured values and the simulation results in the first model layer using a sample cycle based on VDI Guideline 2198. The measured profiles of the engine speed and the pivot angle of the drive pump are used as input data for the simulation. The upper graph shows the vehicle speed, while the lower graph shows the line pressures present at the drive pump in the power lines L1 and L2. The good correlation between the simulation and measurement results means that the simulation is suitable for use in the subsequent development and evaluation of the system, as well as for development of the operating strategy.

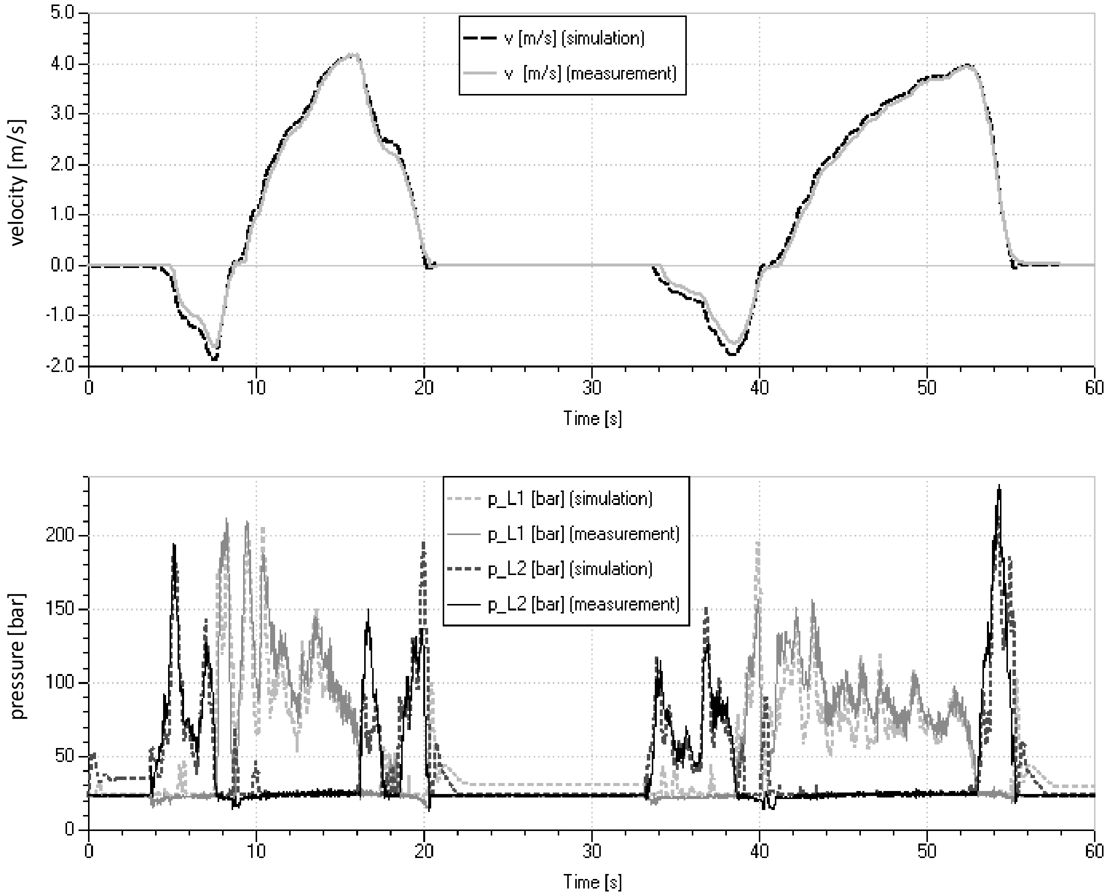

Figure 1: Comparison between the measured values and the simulation results

3 Potential for energy recuperation and fuel and emissions reductions

The fuel consumption of industrial trucks is usually given in the manufacturer data sheets on the basis of the cycle specified by VDI Guideline 2198. Since all manufacturers strive to drive this cycle with minimal fuel consumption of their vehicles, it is a suitable tool for the comparison of different vehicles. However, the cycle does not allow reliable statements to be made about the resulting fuel consumption in normal operation. **Figure 2** shows a comparison of two measured driving cycles, both of which correspond in principle to the cycle specified by the VDI guideline. Using the same route, but with driving time reduced by 25%, the energy demand at the drive pump increases by 50%. At the same time, due to the higher accelerations, the proportion of recoverable energy at the crankshaft (CrSh) can be increased from 5% to 27% of the input energy. This example clearly shows both the influence of driver behaviour on the energy demand and how it affects the potential for recuperation.

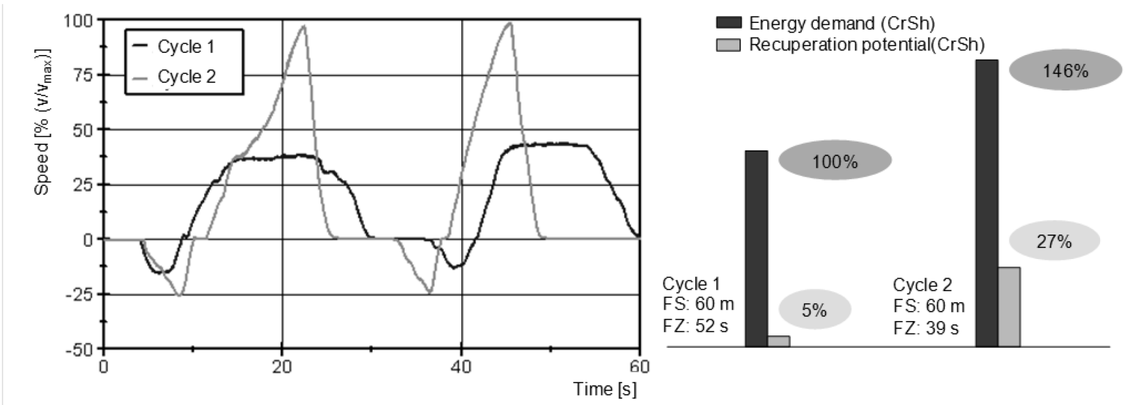

Figure 2: Recuperation potential as a function of driver behaviour

The decelerations that occur during driving operations are critical to the effectiveness of any recuperation measures. **Figure 3** shows the potential for recuperation using calculations based on measured results (engine speed and power line pressures) as observed on the test vehicle. The recuperation potential is determined by dividing the amount of energy recuperated and captured in intermediate storage by the kinetic energy at the start of vehicle deceleration. Recuperation is possible for decelerations as low as 0.4 m/s^2, however, for very small decelerations it is necessary to supply energy to the system.

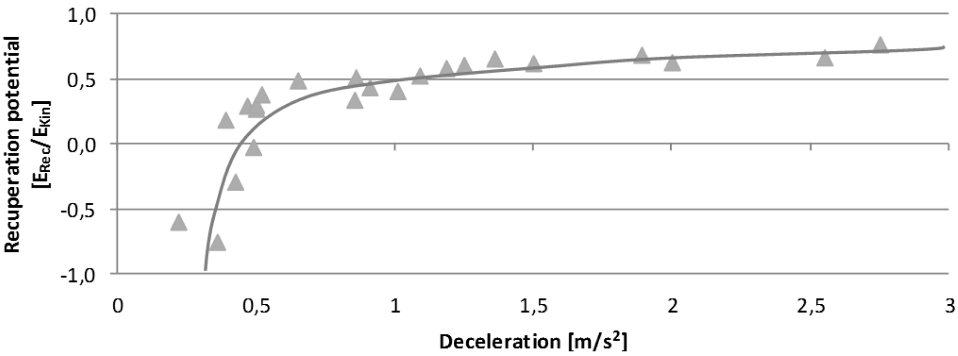

Figure 3: Recuperation potential as a function of deceleration

4 Hydro-mechanical energy storage

Intermediate storage of energy is required in order to make full use of the energy recuperated during vehicle deceleration. This section discusses the conceptual design of the storage system for the hybridisation of the industrial truck considered here.

4.1 Selection of the storage system

Table 1 compares the different storage technologies that can potentially be used in mobile applications.

Storage Technology	Energy density [Wh/kg]	Power density [W/kg]	Number of cycles	Efficiency [%]
Flywheel	5-50	180-1800	10^6	90-95
Battery	30-200	100-700	1000	80-85
Capacitor	2-5	7000-18000	$<10^6$	>95
Bladder	0.2-5	3000-300000	10^6	94

Table 1: Storage technologies /1/, /2/

Most mobile machines are in need of a counterweight in order to allow them to carry out the tasks they are designed to perform. Replacing the counterweight with a storage device opens up the possibility of making active use of this necessary mass. It is apparent then that in this type of application, mass-related energy and power density play a smaller role than in passenger cars. However, the packaging space is highly significant. The storage capacity provided should be at least the same as the maximum kinetic energy stored in the vehicle. In order to allow for the future possibility of storing the potential energy of fork and workload, the storage capacity for the application considered here was set to 30 Wh. In simulations, it was shown that the storage capacity of 30 Wh is also sufficient for phlegmatisation of the internal combustion engine. In addition to this, the storage device must be able to accommodate 40 kW in order to store the energy generated during rapid deceleration. A flywheel is used as the energy storage device for the hybridised industrial truck considered here because it provides a combination of high power and high energy density with low cost.

4.2 Integration into the powertrain

For the powertrain of the industrial truck considered here, during braking, kinetic energy is initially converted into hydraulic energy in the wheel motors. In order to store this energy for use in subsequent acceleration phases, the proposed powertrain incorporates an additional adjustable axial piston unit to convert the energy into mechanical energy for intermediate storage in the flywheel. **Figure 4** shows a schematic representation of the proposed powertrain. During braking, energy is extracted from the system by the additional adjustable axial piston unit and stored in the flywheel. This is then fed back during acceleration in order to reduce the energy input required from the conventional drive pump. This reduces the load on the internal combustion engine, while at the same time allowing it to operate in regions of higher efficiency. Drawing off the energy in the hydrostatic circuit allows conversion losses during recuperation to be reduced compared to systems that draw off energy at the crankshaft. Moreover, the hydraulic connection to the storage device also allows the storage system to be located at any desired position, which, for example, would not be possible in the case of a mechanical coupling of the flywheel to the crankshaft.

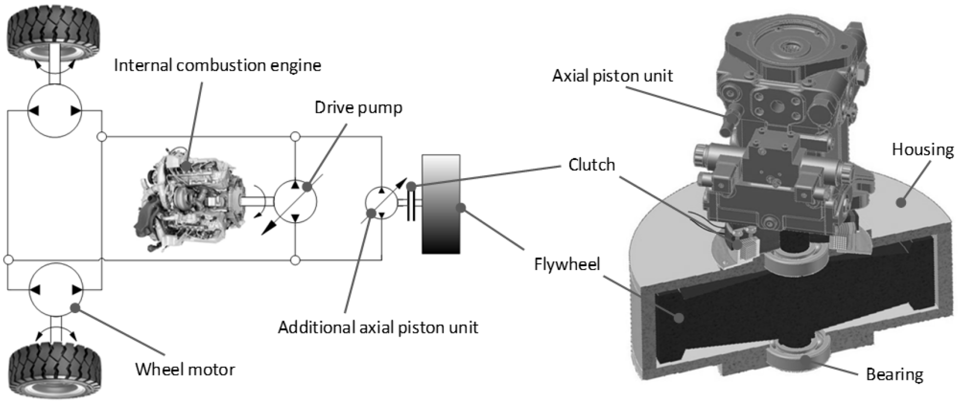

Figure 4: Powertrain layout

4.3 Dimensioning of the axial piston unit

In order to recuperate the full kinetic energy of the vehicle, the flow rate of the additional axial piston unit at minimal flywheel speed must correspond to the resultant volumetric flow rate of the wheel motors at maximum vehicle speed. The size of the pump selected determines the lower limit for the rotational speed range of the flywheel energy storage device. The upper limit is determined by the maximum speed of the pump. In order to achieve the lowest possible rotor weight it is important to provide a sufficiently wide speed range for the flywheel storage device, which means a 56 ccm pump is required (see **Figure 6**). The resulting speed range of 2250-3900 rpm allows 70% of the total storage capacity of the flywheel to be utilised. The maximum speed of 3900 rpm means that this implementation falls into the category of slow-speed flywheel energy storage.

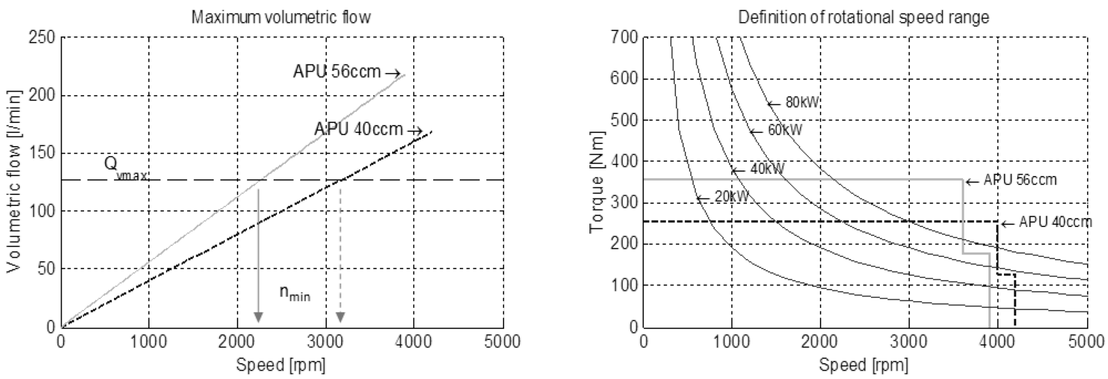

Figure 6: Definition of rotational speed range

4.5 Flywheel design

The most important parameters for dimensioning the storage system are the required storage capacity, the operating speed range and the maximum dimensions. **Figure 5** illustrates the general procedure for designing a flywheel storage. For dimensioning and no-load loss analysis a design tool was implemented, which can be used for different applications by varying the main parameters.

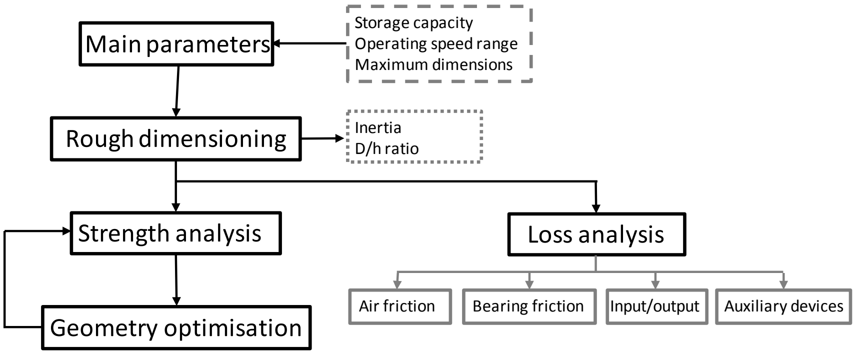

Figure 5: Flywheel storage device design procedure

The useful storage capacity of a flywheel storage device is a product of the flywheel inertia and the usable speed range (1).

$$E_{rotNutz} = \frac{1}{2} J_S (\omega_{S\max}^2 - \omega_{S\min}^2) \tag{1}$$

The moment of inertia required is thus obtained from the defined speed range and the required storage capacity of 30 Wh. In the case considered here, the moment of inertia needed is 1.9 kgm^2. **Table 2** gives the material properties of various flywheel materials. It is clear that there is a significant difference with respect to the energy density achievable when different materials are used. Due to the higher specific strength of fibre-reinforced materials, the achievable energy density is much higher than for metal rotors. This notwithstanding, the system described makes use of a steel rotor. Due to its very low speeds, the benefit to be gained by using a fibre-reinforced rotor would be very small compared to the cost and effort required to implement this.

Material	Tensile strength [MPa]	Density [kg/m3]	Specific strength [kNm/kg]	Max. peripheral speed [m/s]	Poss. energy density [Wh/kg]
Steel	1300	7800	167	410	106
Titanium	1150	5100	225	570	143
GFRP	1300	1900	680	820	335
CFRP	6300	1546	2470	1570	1570

Table 2: Properties of various flywheel materials /3/

Figure 7 shows the rough dimensioning carried out using the main parameters, allowing the user to reach a conclusion about the required flywheel mass based on the diameter chosen.

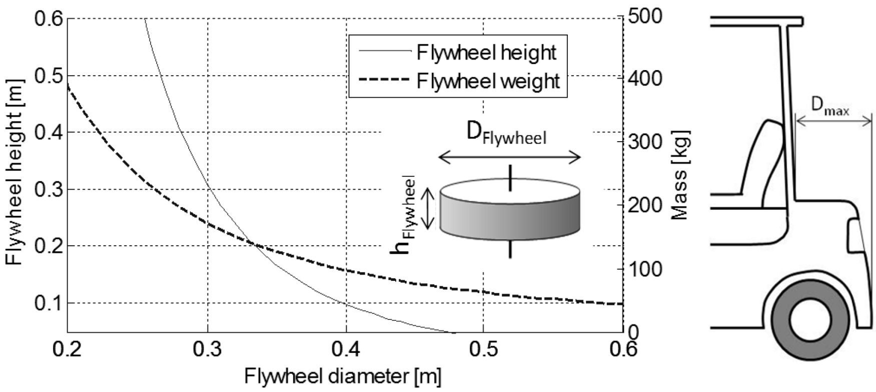

Figure 7: Rough dimensioning of a flywheel storage device

The critical factors in determining the outer diameter are the packaging space available, the weight of the flywheel needed and the limits given by the strength analysis based on material and maximum rotational speed. Due to the restricted packaging space available in the vehicle, for the industrial truck considered here the only option is to mount the energy storage module on the rear of the vehicle. In order to avoid extending beyond the outer boundary of the vehicle footprint, the diameter of the module is limited to 43 cm. The low speeds involved in the application discussed here mean that the stresses are sufficiently low in the available diameter range to allow a metal rotor to be used. During the optimisation phase, the envelope of the rotor can be adapted in order to increase the form factor, that is to achieve uniform material loading and thereby reduce the rotor weight.

4.6 Safety of the flywheel energy store

To protect for the case of a catastrophic failure of the flywheel, it is important that the housing is sufficiently robust to absorb the energy of any pieces that break away. The fracture behaviour of the rotor is key in determining the energy transferred to the wall of the housing. Fibre-reinforced rotors can be dimensioned in such a way as to ensure that they disintegrate into many tiny pieces if a burst occurs. By contrast, metal rotors tend to break into a few large pieces. The key factor for determining the required strength for the housing wall is the height and the proportion of the translational energy in the fragment. This generally depends on the type of rotor construction, but is primarily a function of the size of the fragment. The complete rotor contains a great deal of energy, however, this is purely rotational. A very small fragment has a very high proportion of translational energy at the point of collision, however, carries very little kinetic energy. The maximum translational energy for a fragment in the form of a segment of a circle lies in the angular range 90°-150° /4/, which corresponds to the range for the typical burst characteristics of a metal rotor. **Figure 8** shows the minimum housing wall thickness for this critical case as a function of flywheel diameter, with storage capacity and air gap held constant as shown in /4/.

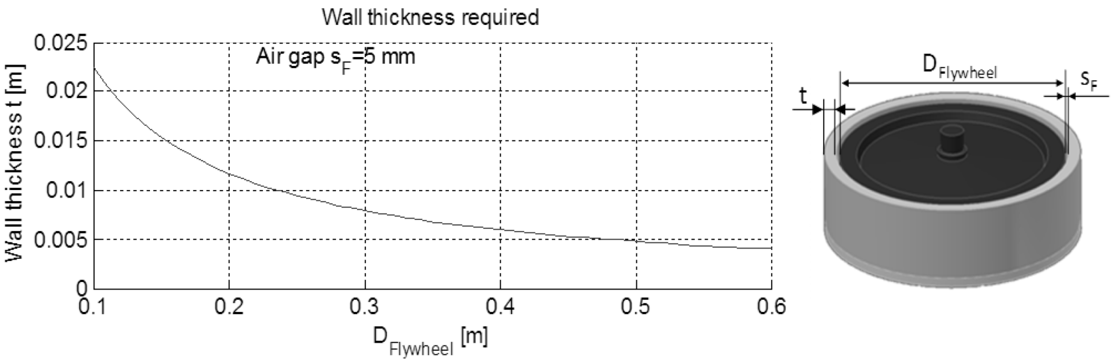

Figure 8: Minimum housing wall thickness required /4/

4.7 Investigation of no-load losses

The overall system efficiency is largely determined by the losses from the storage system. Losses can be categorised into types as follows: flywheel losses (air friction, bearing friction), input/output losses and energy demand from auxiliary loads (e.g. vacuum pumps, control systems).

The gas friction losses, P_{GF}, can be estimated using Equation (2) /5/, which assumes turbulent gas flow and enclosed operation.

$$P_{GF} = 3.64 \cdot 10^{-2} \cdot R_F^{4.6} \cdot \rho_G \cdot v_G^{0.2} \cdot \omega_F^{2.8} \left(1 + 0.82 \cdot h_F \cdot s_F^{-0.3} \cdot R_F^{-0.7} \right) \quad (2)$$

Figure 9 illustrates the power dissipation as a result of gas friction for various flywheel diameters, $D_{Flywheel}$, as a function of rotational speed, as well as the effects of system pressure on the losses due to gas friction. Lowering the system pressure to 0.1 bar corresponds to a reduction in losses due to gas friction of 85%. In contrast, however, there are additional energy losses as the result of operating a vacuum pump and additional losses due to a more complex sealing system.

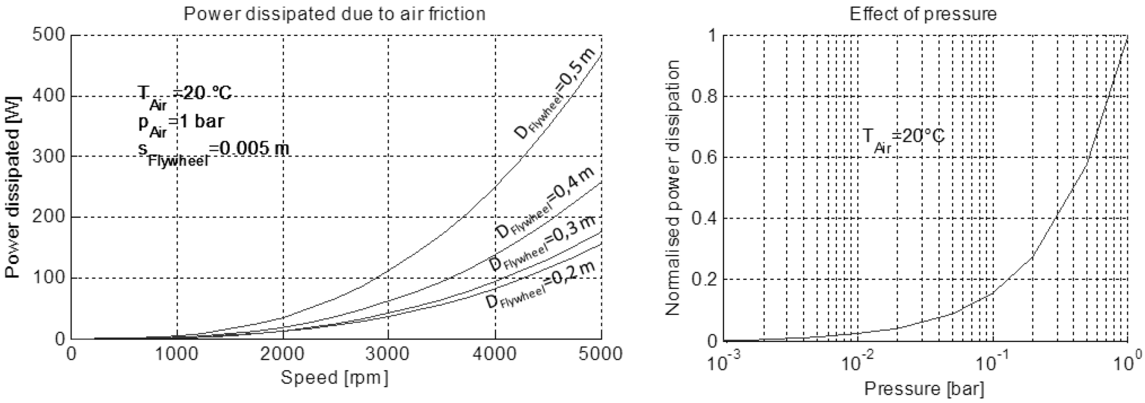

Figure 9: Power dissipation as a function of speed, flywheel diameter and system pressure

The choice of bearing has a major influence not only on the losses, but also on maintenance intervals and, therefore, on the availability of the vehicle. Because of the cost/benefit ratio, magnetic bearings are not an option for this application. An estimate can be obtained of the losses from roller bearings using the formulae specified in /6/ or Equation (3) /5/, which already includes an experimentally determined correction factor.

$$P_{BF} = \omega_F \cdot \sum_{i=1}^{n} \frac{D_{Bgi}}{2} \cdot \mu_{Bgi} \cdot x_{LBgi} \cdot \left(m_S \cdot \sqrt{g^2 + e^2 \cdot \omega_F^4} + 5.6 \cdot \omega_F \right) \qquad (3)$$

Substantial losses result from direct coupling of the axial piston unit and the flywheel during no-load phases. Even with a differential pressure of 0 bar the losses by dragging the pump are higher than 1 kW. In order to eliminate this effect, a decoupling mechanism has to be integrated between the pump and the flywheel (**Figure 4**). This means that the losses in the storage device during no-load phases are then only due to gas and bearing friction. **Figure 10** shows the characteristics of the hybridisation system designed for this application, along with estimates of resultant no-load losses.

Flywheel energy storage device	Capacity	30 Wh
	Maximum speed	3900 1/min
	Useful speed range/Max. speed	42 %
	Material	Steel
	Moment of inertia	1,9 kgm²
	Diameter	380 mm
	Quality of balancing	G 6,3
Bearing	Roller bearing	
Input/output	56 ccm swash plate pump	
Clutch	Tbd.	
Vacuum pump	Coarse vacuum (250mbar)	

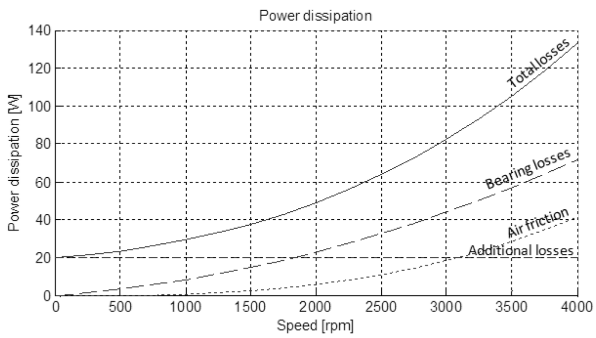

Figure 10: Characteristics of the designed system

5 Summary and outlook

A new hybrid system for a forklift truck, which according to simulations can realise energy savings of up to 14% using brake energy recuperation, has been presented. A flywheel is used for energy storage, which is integrated with the existing closed hydraulic circuit by means of an additional axial piston unit. Components have been dimensioned and system safety and no-load losses have been optimised. The concept is transferable to other types of applications and systems. The next phase in development will focus on detailed design and geometry optimisation. The flywheel storage device will be designed and manufactured based on the results. In parallel, the operating strategy will be developed based on the validated version of the vehicle model created. Fuel consumption measurements will be made once the system has been implemented in the target vehicle in order to test the plausibility of the simulated fuel reductions.

EUROPÄISCHE UNION
Investition in unsere Zukunft
Europäischer Fonds
für regionale Entwicklung

Ministerium für Wirtschaft, Energie,
Bauen, Wohnen und Verkehr
des Landes Nordrhein-Westfalen

7 Bibliography

/1/ Dr. T. Anderl, Energieeffiziente Antriebskonzepte für mobile Arbeitsmaschinen, Colloquium HDTC – Opening by IME, Aachen, 2010

/2/ Energiespeicherung für elektrische Netze, VDI-Gesellschaft Energietechnik, VDI Report 1404, VDI Verlag, Düsseldorf, 1998

/3/ Dr. P. von Burg, Moderne Schwungmassenspeicher – eine alte Technik in neuem Aufschwung, VDI-GET Fachtagung Energiespeicherung für elektrische Netze, 10-11 November 1998, Gelsenkirchen, Germany

/4/ G. Genta, Kinetic Energy Storage, Butterworths & Co, Great Britain, 1985

/5/ J.W. Biermann, Untersuchung zum Einsatz von Schwungradenergiespeichern als Antriebselemente für Kraftfahrzeuge, Dissertation, Aachen, Germany, 1981

/6/ SKF: http://www.skf.com/portal/skf/home/products?maincatalogue=1&lang=de &newlink=1_0_40 (accessed November 2011)

8 Nomenclature

E_{Rot}	Rotational energy	Ws

J_F	Moment of inertia	kg m^2
ω_F	Angular velocity	1/s
R_F	Rotor radius	m
h_F	Flywheel height	m
s_F	Air gap	m
t	Thickness of housing wall	m
v_G	Kinematic viscosity	m^2/s
ρ_G	Gas density	kg/m^3
D_{Bg}	Average bearing diameter	m
μ_{Bg}	Coefficient of friction of bearing	
X_{Bg}	Bearing load factor	
m_F	Flywheel mass	kg
g	Acceleration due to gravity	m/s^2
e	Rotor eccentricity	m